Photoreflectance characterization of ultrashallow junction activation in millisecond annealing

Will Chism[a)]
Xitronix Corporation, 3925 W. Braker Lane, Third Floor, Austin, Texas 78759

Michael Current
Current Scientific, 1729 Comstock Way, San Jose, California 95124

Victor Vartanian
International Sematech Manufacturing Initiative, 257 Fuller Road, Ste. 2200, Albany, New York 12203

(Received 15 June 2009; accepted 28 September 2009; published 1 March 2010)

Photoreflectance (PR) provides an optical means for rapid and precise measurement of near-surface electric fields in semiconductor materials. This article details the use of PR to characterize dopant activation in ultrashallow junction (USJ) structures formed using millisecond annealing processes. USJ structures were formed in silicon using 500 eV B implantation with a dose of $10^{15}/\mathrm{cm}^2$, followed by flash anneals at 1250–1350 °C. Reference metrology was performed using secondary ion mass spectrometry and various sheet resistance (R_s) methods. Methods to calibrate PR signals to active carrier concentration in USJ structures, including halo-doped samples, are described. PR is shown to be highly sensitive to active dopant concentrations in USJ structures formed by millisecond annealing. © *2010 American Vacuum Society.* [DOI: 10.1116/1.3253327]

I. INTRODUCTION

The advent of millisecond ultrashallow junction (USJ) annealing processes has enabled very high levels of USJ activation with minimal dopant diffusion. However, residual damage remaining after millisecond annealing increases the junction leakage, particularly for junctions formed with highly doped halo profiles.[1] Thus, it is necessary to monitor activation and leakage currents for USJs, especially those formed with highly doped halo profiles. Current millisecond annealing process technologies use scanned laser beams or flash-lamp arrays. Either approach may introduce microscale variability to the dopant activation since patterned films present at the annealing step cause variations in the amount of light absorbed in the underlying silicon. Also, in the case of a laser anneal, microscale variability is introduced by the stitch overlap between laser scans and/or the interference effects in the projected laser intensity distribution.[2] Thus, the ideal process control technique must provide fast "on-product" measurement capability with microscale resolution.

Many existing measurement techniques such as secondary ion mass spectroscopy (SIMS) have time and/or material limitations that render them unsuitable for process control of USJ activation in millisecond annealing. Also, for macroscopic four-point probe techniques, high leakage current densities make it impractical to measure sheet resistance (R_s) of USJs formed with highly hoped halo profiles.[1,2] Carrier spreading and recombination methods, such as surface photovoltage, provide noncontact activation (R_s) and junction leakage measurements but with limited ($\approx 1\ \mathrm{mm}^2$) spatial resolution.[3] Other techniques are sensitive to damage but not electrical activation and, therefore, provide only partial information.[3]

However, photoreflectance (PR) is a powerful tool to study the electric field distribution at semiconductor interfaces, such as those occurring at USJs.[4,5] In PR, the semiconductor electric field distribution is modulated by the photoinjection of electron-hole pairs using an amplitude-modulated pump light beam.[5,6] The semiconductor reflectivity is monitored with a probe light beam. For probe wavelengths that are resonant with semiconductor interband transitions, the PR signal arises from an electromodulation effect.[4–7] This provides a means for optical detection of semiconductor electric fields through the appearance of sharp, third derivative spectra.[7,8] Since PR measures the change in the reflectivity of the semiconductor structure in response to the ac electric field, there also exists important information in modulation parameters such as pump intensity, wavelength, and modulation frequency.

In this article, we report the application of PR technology to characterize electrical activation in USJ structures formed by flash anneal, including highly doped halo profiles both with and without preamorphization implants (PAIs). The PR technology described here utilizes a probe laser beam of 375 nm wavelength, which is near the Si "E_1" interband transition energy. This probe wavelength is ideal for characterization of electric fields occurring in advanced silicon USJs.[9] The absorption depth of the probe light in silicon, given by $\delta \equiv 1/\alpha = (4\pi k/\lambda)^{-1}$, is approximately 23 nm. The wavelength of the amplitude-modulated pump laser beam is 844 nm and the pump modulation frequency is 2 MHz. The pump and probe lasers operate at milliwatt powers and are cofocused to a spot of approximately 6 μm at the sample surface. We report PR measurements of USJ electromodulation arising from modulation of the junction field. The use of the PR technique for rapid and precise characterization of

[a)]Electronic mail: wchism@xitronixcorp.com

millisecond annealing processes, including the halo preanneal, is demonstrated. Sensitivity of PR to residual junction damage is also discussed.

II. PRINCIPLES OF PHOTOREFLECTANCE MEASUREMENT

Modern PR techniques are routinely used to measure differential changes in reflectivity smaller than 1 ppm. Accordingly, they are an ideal candidate for applications, requiring measurement of small optical signals related to electronic transitions in semiconductor nanostructures. In PR, a pump laser beam is used to periodically modulate the carrier density in a semiconductor sample, and hence modulate one or more physical quantities, such as internal electric fields and interband transition energies, thereby inducing a periodic variation in the reflectivity of the sample, which is then recorded by the use of a coincident probe light beam.

As mentioned, the PR metrology technique discussed herein attains sensitivity to the active electronic properties of Si nanostructures by using a probe wavelength near the E_1 interband transition in Si, which occurs at a wavelength of approximately 375 nm. Near this transition, the PR signal may be written as

$$dR/R = F^2 \times L(h\nu), \tag{1}$$

where dR/R is the normalized change in reflectivity, F is the internal electric field, and $L(h\nu)$ is a line-shape function determined by the semiconductor band structure, where h is Planck's constant and ν is the photon frequency $(\nu = c/\lambda)$.[8,10]

One motivation for selecting the wavelength of the probe beam at 375 nm lies in the sharp derivative form for $L(h\nu)$. In particular, this line-shape function has a third derivative from near strong optical absorptions in the semiconductor band structure and thus may be utilized to isolate these features with great precision. This enables the PR technique to precisely measure strain in nanoscale strained silicon layers, for example, since the Si E_1 transition energy undergoes a known shift under strain.

Near these strong optical absorptions, the amplitude of the PR response also has excellent sensitivity to space charge fields in USJs. The Poisson relation may be used to estimate the space charge field at the junction: $F^2 \cong -2eN_eV/\varepsilon_0$, where e is the electronic charge, N_e is the active doping concentration, V is the built-in potential, and ε_0 is the static dielectric constant. The physical situation of the USJ under pump illumination is equivalent to that of a p-n photodiode under illumination.[11,12] To better understand the carrier dynamics influencing the PR signal, Fig. 1 shows a schematic energy band diagram of a p-type USJ structure. Figure 1 also shows the schematic carrier flow when the pump beam is on (upper) and when the pump beam is off (lower). The pump beam absorption depth in silicon is of the order of microns, which provides an effectively uniform distribution of photoinjected carriers over the probe sampling depth. When the pump laser is on, photogenerated carriers at the junction separate in the built-in electric field at the junction and reduce the field. This produces a forward bias condition. When

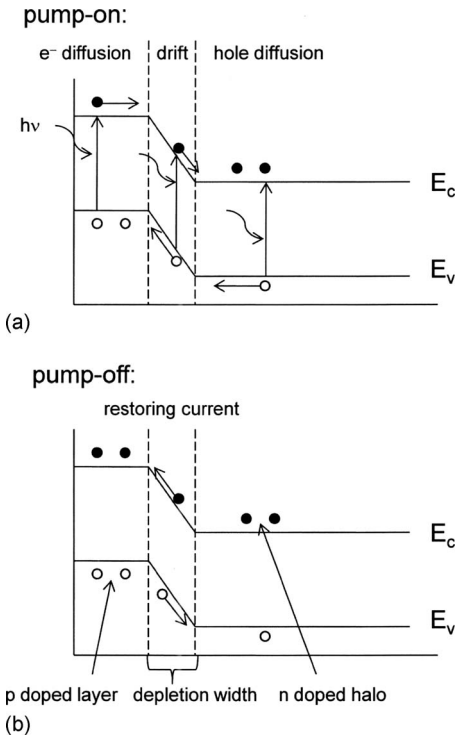

FIG. 1. Schematic energy band diagram of a p-type USJ for (a) pump laser on and (b) pump laser off. Carrier recombination and tunneling effects are not included here for clarity.

the light pump is switched off, the electric field returns to its built-in value by a restoring current. The p-n junction current density is determined by drift current due to carriers created within the depletion region and by a diffusion current due to carriers generated outside the depletion layer. In USJs the contribution of the diffusion current is small in comparison to the drift current due to carriers within the depletion width.[11] The presence of defects in the junction depletion layer greatly enhances carrier recombination and tunneling effects, resulting in leakage currents, which also reduce the junction potentials. The transit time for carriers to traverse the depletion layer is less (and often much less) than the modulation time scale. Thus, the PR signal (at 375 nm) corresponds to the reflectivity difference between two steady state conditions, i.e., the junction electric field with pump on versus pump off. The experimentally measured PR signal then becomes

$$dR/R \cong -2eN_e\Delta V/\varepsilon_0 \times L(h\nu), \tag{2}$$

where ΔV is the photovoltage induced by the pump at the junction.[5,8] Accordingly, in the case of a shallow junction located within the absorption depth of the probe, the PR signal will be linearly proportional to active doping concentration.

Additionally, because the pump amplitude modulation occurs at at megahertz frequencies, the recombination contribution to the bulk current is expected to be small or negligible. In particular, at megahertz modulation frequencies, the bulk diffusion current depends essentially on the mobility, with small or negligible contribution from bulk

recombination.[13] In this case, the bulk diffusion current arises from the redistribution of charges initially located within the carrier diffusion length $\cong(D/\Omega)^{1/2}$, where D is the ambipolar diffusion coefficient and Ω is the modulation frequency.[13] However, the PR signal will depend on the residual damage through its effect on drift current in the depletion region due to the dependence of junction photovoltage on defect density in the depletion layer.[3,11]

III. MEASUREMENT RESULTS AND DISCUSSION

Millisecond anneals were performed using flash annealing processes where the wafer is rapidly heated to an intermediate temperature (700–750 °C) and its front surface is then heated (to 1250–1350 °C) by a millisecond duration pulse of energy from a flash-lamp array. USJ structures were formed using 500 eV B implantation with a dose of $10^{15}/\mathrm{cm}^2$, followed by flash anneals at 1250–1350 °C. The wafers were crystalline silicon (100) oriented, n-type with resistivity approximately 10–15 Ω cm. The process matrix included PAI and halo doping splits including preannealing the halo implant prior to implanting the USJ. The PAIs were 10^{15} Ge/cm^2 at 30 keV and the halo implants were 4×10^{13} As/cm^2 at 40 keV. In a subset of the samples, the halo implants were preannealed for 10 s at 1050 °C prior to the PAI or B implants.

We compare PR data with activation levels estimated from R_s and SIMS measurements. The results show that PR measurements are effective to monitor USJs formed in halo-doped profiles, including cases where leakage current makes four-point probe data unreliable. Further, we delineate the effect of preannealing on the halo-doped samples and show the impact of residual damage at the junction on the PR measurement. For the heavily damaged junctions of the PAI samples, the halo condition is shown to have little impact on the PR response.

The experimentally measured PR signal consists of a vector characterized by an amplitude and a phase. The PR amplitude is $|dR/R|$, the induced change in reflectivity (ac) divided by the reflectivity (dc). The amplitude and sign of the PR vector determine the relative change in the probe reflectance due to the modulated electric field distribution. For the majority of samples reported herein, the PR vector measurement is in the lower right quadrant. Based on the details of the PR apparatus, this simply means the probe beam reflectivity decreases under the "pump on" condition. This vector direction is typically observed for p-type substrates, although with a much smaller vector amplitude (due to the smaller built-in fields). Conversely, for n-type substrates, the probe reflectivity typically increases under the pump-on condition (phase in the upper left quadrant). The reason for this difference is that the pump-on condition always reduces the built-in field, thus the sign of the photoinduced change in potential ΔV is opposite for p-type versus n-type substrates, which manifests itself in the observed PR signal as a change in sign. The PR phase corresponds to the rise and decay times for the reflectivity changes, i.e., the PR vector phase measures the semiconductor response time required to reach steady state, relative to the inverse driving frequency. The electronic delay of the PR detection system is roughly −10° (with respect to the x axis). Thus, a measured phase of approximately −70° corresponds to a physical phase of approximately −60°, which implies a semiconductor response time of the order 0.1 μs.

Figure 2 shows the measured PR vector for the USJ halo-doped samples with no PAI. The solid points are the measured PR vectors on halo-doped samples without halo preanneal. The open points correspond to the flash-annealed halo-doped samples with preanneal. The only difference in process conditions between the sample sets is the preannealing of the halo. Also plotted in Fig. 2 are the PR data for wafers without the halo or PAI (denoted as X). The detected electromodulation on these samples is two orders of magnitude smaller than that observed on the halo-doped samples, irrespective of flash annealing conditions. This is consistent with the estimated electrical junction depths of approximately 100 nm (without halo), below the sampling depth of the probe. The data labels correspond to the peak flash annealing temperature or process.

The PR data on halo-doped samples is remarkable in several aspects. First, by looking at the series of PR measurements for the halo without preanneal (solid points), it is seen that the PR vector amplitude increases in response to a higher flash annealing temperature. The increasing PR amplitude is indicative of sensitivity to activation since for flash annealing processes the activation depends on the peak process temperature. The PR amplitude also responds to the integrated flash time: the 2X (repeated) 1300 °C flash process produces a PR measurement very similar to the 1350 °C flash condition. Figure 3 shows the PR amplitude for the flash-annealed USJ halo-doped samples (without a halo preanneal) plotted versus the effective time for B diffusion,[1] which here serves as a convenient measure of the flash anneal thermal budget. The effective time of an anneal is the time a sample would have to spend at a reference temperature, usually chosen to be 1050 °C, to produce the same process effect, usually taken to be the dopant diffusion length with boron activation and 3.46 eV. The PR signal is seen to vary linearly with the effective time. The linearity of the measured PR data with flash effective time is a consequence of the linear dependence of the PR signal on the activation level.

Another feature evident in Fig. 2 is the high degree of correlation between the data distribution from the "preannealed halo" sample set and the distribution from the flash-annealed halo (the distribution of PR data within either set shows the PR signals responding to B activation). The primary difference in the observed distribution of the preannealed halo samples is an overall shift of the PR vector. This shift is consistent with greater n-type activation and illustrates that the PR signal is responding to the halo activation. The distribution of the measurements on samples with a halo preanneal is also scaled with respect to the PR distribution on the samples without a halo preanneal. While the vector shift of the preannealed halo data implies greater halo acti-

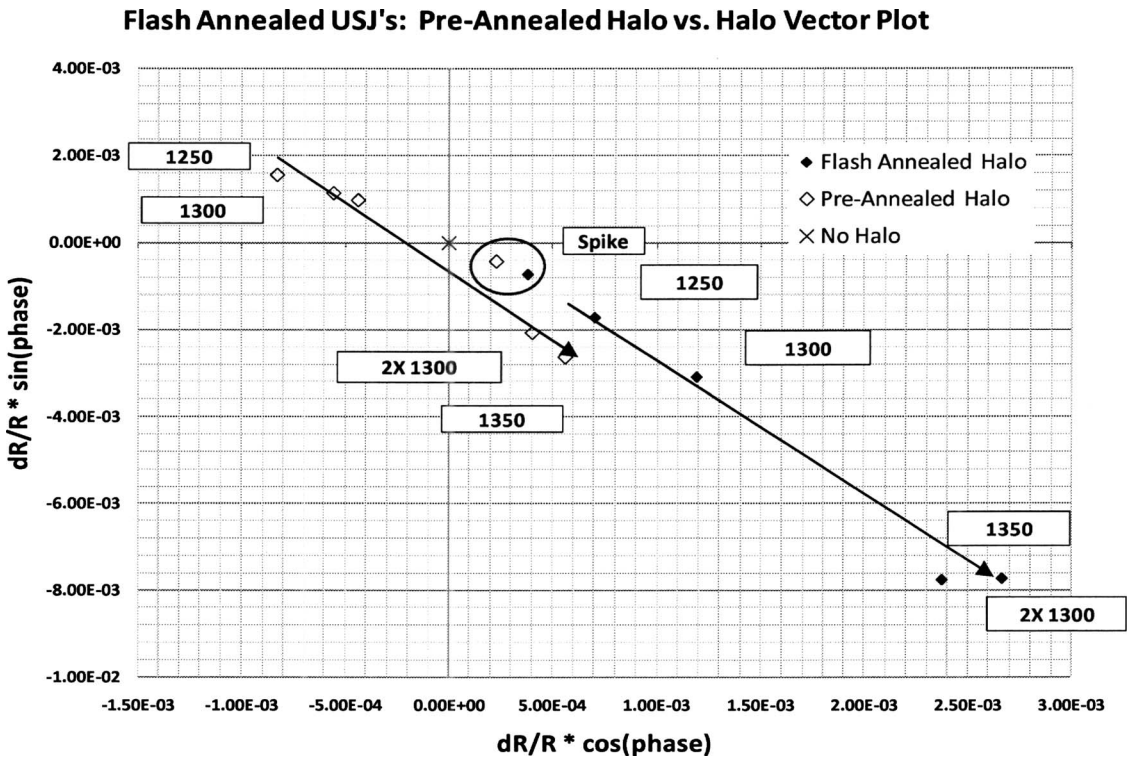

FIG. 2. Measured photoreflectance vector for the USJ halo-doped samples (no PAI).

vation, the scaling of the observed PR amplitude on the preannealed halo samples is consistent with reduced junction leakage (due to the lower residual damage) resulting in smaller junction electromodulation.

Figure 4 further illustrates the sensitivity of PR to residual damage at the junction. Figure 4 shows the measured PR vector for the USJ halo-doped samples with PAI. The set of points denoted by "PAI, halo" correspond to samples that have PAI and halo, and the set of points denoted by "PAI, AH" correspond to samples that have PAI and a "preannealed" halo. The data labels correspond to the final flash annealing temperature. The PR datasets are seen to be closely paired according to the flash process conditions. For each pair of points, the only difference in process conditions is again the preannealing of the halo prior to PAI. In this case, any reduction in residual damage due to the halo preanneal is obscured by the heavy damage from the PAI. The close proximity of the pairs of points shows that the PR measurement produces similar values on similar USJs with similar (heavy) damage profiles; i.e., the PR measurements are consistent with the residual damage at the junction being determined primarily by the PAI. The PR vector translates with USJ flash annealing temperature, again indicating a high degree of correlation of the PR signal with activation. Also plotted are the PR data for wafers with PAI but no halo (denoted by *X*). The detected electromodulation on these samples is two orders of magnitude smaller than that on the halo-doped samples, consistent with an electrical junction depth below the sampling depth of the probe. Here, the 1350 °C flash-annealed samples were also dramatically shifted with respect to the distribution, indicating a process difference common to either wafer. In this case, the process conditions have induced strain, which is observed in the PR measurement by and through its dependence on the lineshape function $L(h\nu)$. Also, a reduced PR phase (faster junction response time) is observed on either halo sample with PAI when subject to the 2*X* (repeated) 1300 °C flash anneal. This reduction in PR phase is consistent with lower levels of residual junction damage being achieved at higher flash temperatures. The effect of the halo preanneal condition is observed in this case, implying the dominant contribution to the residual junction damage after the repeated 1300 °C flash anneal arises from the halo implant. Otherwise the distribution of PR data shows that the junction profile and damage conditions are similar for a given PAI/flash condition irrespective of the halo preanneal. This demonstrates that the

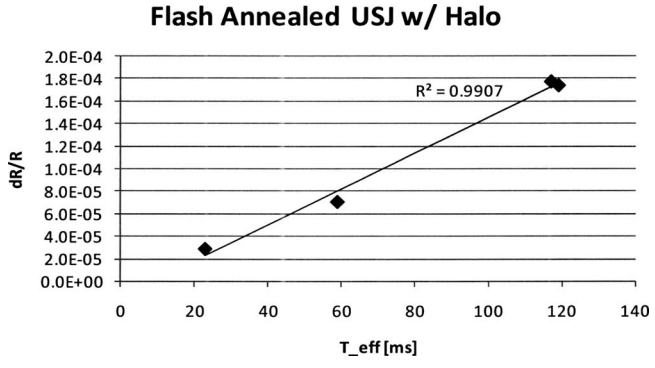

FIG. 3. Photoreflectance signal plotted vs flash effective annealing time.

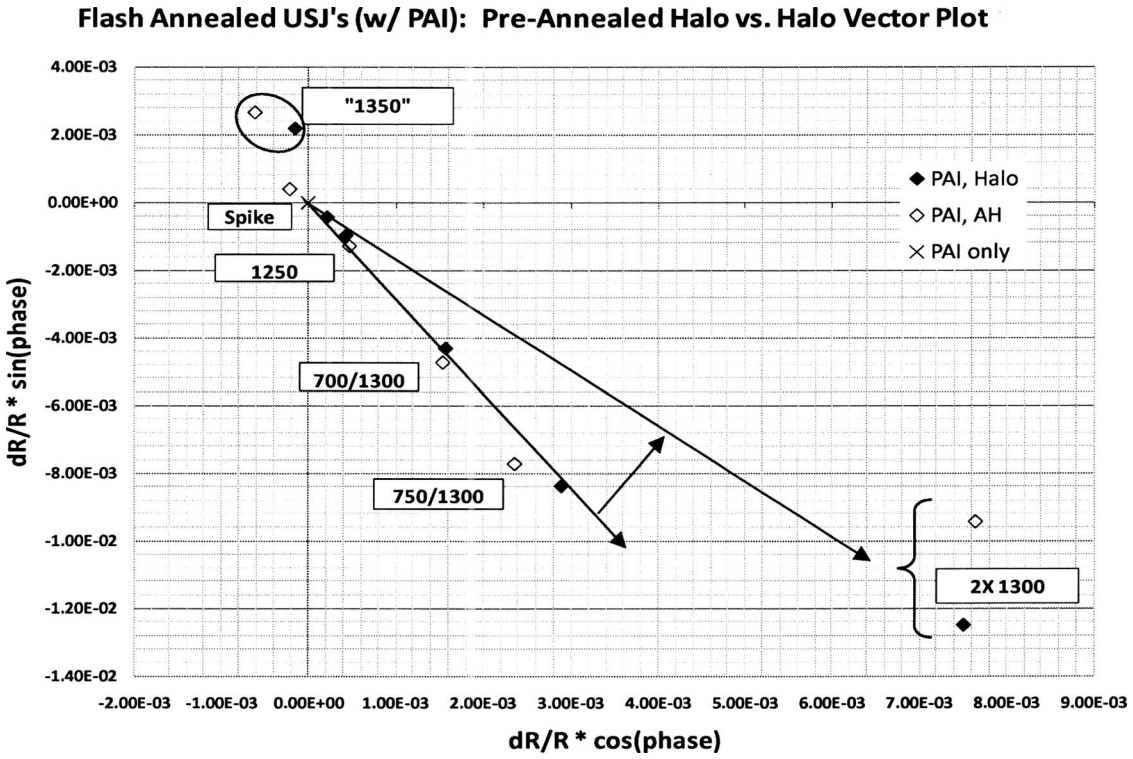

FIG. 4. Measured photoreflectance vector for the USJ halo-doped samples with PAI.

primary source of residual junction damage is the PAI implant for flash anneals below 1300 °C (single flash).

Figure 5 shows the PR amplitude for the flash-annealed USJ halo-doped samples with PAI plotted versus the effective annealing time (here, the 1350 °C data have been omitted).[1] The PR signal is again highly linear with effective annealing time. The linearity to USJ activation is shown in Fig. 6. Here, the PR signal is plotted versus activation levels, as estimated from combining R_s and SIMS measurements.[1]

In summary, we have observed PR signals arising from modulation of the junction electric field in halo-doped USJ structures. The amplitude of these signals is observed to be linearly proportional to the active dopant concentration, as predicted. Further, the negligible signals observed on the samples without halo demonstrate the PR signal does not arise from conventional thermal or plasma (Drude effect) modulation.[13] Thus, these complications are avoided. The PR data distribution on the "preannealed halo" structures is uniformly shifted with respect to the "halo without preanneal" distributions and demonstrates the PR sensitivity to halo activation. The overall similarity between observed PR measurement distributions on the two PAI sets (and the "halo without preanneal") confirms the PR is probing the electrical effect of defects at the junction. This point is confirmed by surface photovoltage results showing orders of magnitude smaller recombination leakage for the pre-annealed halo samples with respect to the PAI samples.[1] Further work is underway to establish the detailed model of the effect of the residual damage at the junction on PR.

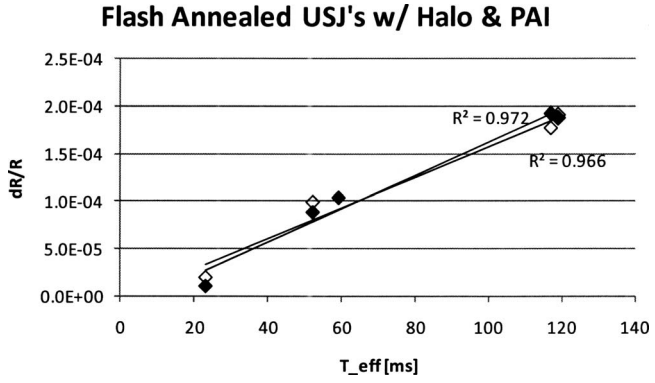

FIG. 5. PR signal plotted vs flash effective annealing time.

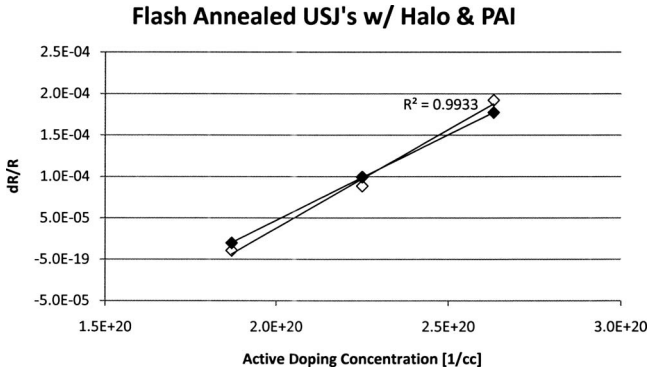

FIG. 6. PR signal plotted vs activation levels for the USJ halo-doped samples with PAI.

Precision studies show that the PR measurement standard deviation is approximately ~1.25% for activation levels approaching the solid solubility limit. In particular, a linear relationship between PR signal and dopant activation has been established for the halo-doped USJs. The sensitivity is the change in the PR signal divided by the change in the active dose. The active dose precision is the PR measurement precision divided by the sensitivity, which is slightly less than $10^{18}/\mathrm{cm}^3$. This resolution is achieved using a measurement time of 3 s, which enables throughputs of approximately 20 wafers/h with 49-point topological maps or with 25-point on-product measurements acquired using pattern recognition.

IV. CONCLUSION

We have reported the application of PR technology to characterize electrical activation in USJ structures formed using millisecond annealing processes. The PR technique is a rapid and practical means to characterize activation in halo-doped USJs, which have depletion regions near the surface. The PR technique provides for sensitive optical detection of USJ electric fields through the modulation of the junction electric field. The sensitivity of PR to residual halo damage at the junction was also reported. With the heavy residual damage from PAI, the prior halo conditions make little impact on the PR response. In summary, the PR technique provides fast on-product measurement capability of junction activation and damage effects with microscale resolution.

ACKNOWLEDGMENT

The authors would like thank Mattson Technology, Inc., for providing USJ samples and reference measurements and to acknowledge valuable discussions with Paul Timans.

[1]P. Timans, Y. Z. Hu, J. Gelpey, S. McCoy, W. Lerch, S. Paul, D. Bolze, and H. Kheyrandish, Mater. Res. Soc. Symp. Proc. **1070**, 1070-E04-03 (2008).
[2]D. H. Petersen, R. Lin, T. M. Hansen, E. Rosseel, W. Vandervorst, C. Markvardsen, D. Kjaer, P. F. Nielsen, J. Vac. Sci. Technol. B **26**, 362 (2008).
[3]Michael Current, Pierre Eyben, Peter Nielsen, Mark Benjamin, Edward Tsidilkovski, Alex Salnik, Andrzej Buczkowski, Tom Kelly, Nobuyuki Ikarashi, in *Ion Implantation Science and Technology*, 2008 ed., edited by J. F. Ziegler (Ion Implantation Tech. Press, Chester, MA, 2008).
[4]H. Shen, F. H. Pollak, J. M. Woodall, and R. N. Sacks, J. Vac. Sci. Technol. B **7**, 804 (1989).
[5]H. Shen and F. H. Pollak, Phys. Rev. B **42**, 7097 (1990).
[6]H. Shen, M. Dutta, R. Lux, W. Buchwald, L. Fotiadis, Appl. Phys. Lett. **59**, 321 (1991).
[7]H. Shen, Z. Hang, S. H. Pan, and F. H. Pollak, Appl. Phys. Lett. **52**, 2058 (1988).
[8]D. E. Aspnes, Phys. Rev. Lett. **28**, 913 (1972).
[9]D. E. Aspnes and J. E. Rowe, Solid State Commun. **8**, 1145 (1970).
[10]D. Aspnes, in *Handbook on Semiconductors*, edited by M. Balkanski (North-Holland, Amsterdam, 1980), Vol. 2, p. 109.
[11]V. N. Faifer, M. I. Current, T. M. H. Wong, and V. V. Souchkov, J. Vac. Sci. Technol. B **24**, 414 (2006).
[12]S. M. Sze and Kwok K. Hg, *Physics of Semiconductor Devices*, 3rd ed. (Wiley, New York, 2007), p. 675.
[13]J. Opsal and A. Rosencwaig, Appl. Phys. Lett. **47**, 498 (1985).